

# New Infrared Photonic Lattice Coating

C.F. Schmidt, W.C. Sweatt, I. El-Kady, F.B. McCormick, D.W. Peters, S.H. Kravitz, J.C. Verley, U. Krishnamoorthy, D. Ingersoll, W.G. Yelton, G. Subramamia, J.D. Williams  
 Sandia National Laboratories, PO Box 5800 MS 1082, Albuquerque, NM USA 87185

## ABSTRACT

We have designed, fabricated, and tested large sheets of photonic bandgap (PBG) material that have a “cubic array of cubes” structure. Structures with bandgaps in two wavebands have been fabricated: the thermal IR (8-12 $\mu$ m) and the visible/near IR (0.6-2.5 $\mu$ m). A thermal-IR PBG can modify the emission properties of structures for temperature control. Visible/near-IR PBGs can be used in photonic circuits and can improve illumination efficiency.

**Keywords:** photonic bandgap structure, mid-infrared, fabrication, contact lithography, nano-imprinting

## 1. INTRODUCTION

In a quest to fabricate large sheets of photonic bandgap (PBG) material we have modeled, fabricated, and tested two “cubic array of cubes” PBG structures<sup>1,2</sup>. One has a bandgap in the thermal IR (8-12 $\mu$ m) and the other’s bandgap is in the visible/near-IR. The thermal-IR development was driven by interest in large pieces of full-bandgap, three-dimensional PBG material that can be used to modify the emissivity of surfaces in the thermal IR for energy scavenging, satellite temperature control, etc. Others are interested in the push toward the visible-NIR operating regimes for use in photonic circuits and to improve the efficiency of illumination systems.

We chose the cubic-array-of-cubes structure<sup>2</sup> (Fig. 1) because it contains the largest features for a given wavelength of operation. For example, a PBG with a 7 $\mu$ m cutoff wavelength requires 2.5 $\mu$ m cubes as compared with feature sizes of  $\approx$ 1 $\mu$ m in logpile and other PBG designs. The 2.5X larger feature size relative to the unit cell dimension (which is proportional to the cut-off wavelength) implies that with a given lithography scheme with a minimum feature size, PBGs can be built for shorter wavelengths. Another major simplification associated with a “cubes” PBG is the reduced number of layers in comparison to logpile photonic crystals. With a cubic array of cubes, a structure that is three unit cells thick takes four layers of cubes, or four mask or nano-imprinting steps. A logpile PBG made with standard lithographic fabrication methods takes twelve mask steps for three unit cells.

Our first thermal-IR PBG is a cubic array of gold cubes in a low-density polyethylene<sup>2</sup> matrix. The structure is one unit cells (2 cubes) thick with 2.5 x 2.5 x 0.5 $\mu$ m gold cubes in a 4 $\mu$ m square matrix. It has a full bandgap that is about 1.5 $\mu$ m wide with a cutoff wavelength near  $\lambda = 8\mu$ m. We are using nano-imprint technology to form each layer of cubes. After the gold cubes are formed and the imprint resist is removed, a 4 $\mu$ m layer of low-density polyethylene is deposited on the substrate encapsulating the cubes and creating the “floor” for the next layer. This process was repeated (using Moire alignment) to create the second layers of cubes as well as subsequent layers. We expect to complete a four-layer structure with three unit cells through the thickness very soon which will have improved reflective characteristics.

The visible/near-IR PBG will be a cubic array of gold cubes in a polyethylene matrix. The 0.26 x 0.18 x 0.2 $\mu$ m cubes are formed on 0.43 $\mu$ m centers giving a bandgap near 900nm. Again, the 2D cube pattern is formed using nano-imprinting and then immersed in a 430nm thick layer of polyethylene. To date we have only created a single layer of cubes for the visible/near-IR. During the fall of 2006 we will fabricate a multi-layer visible/n-IR PBG.

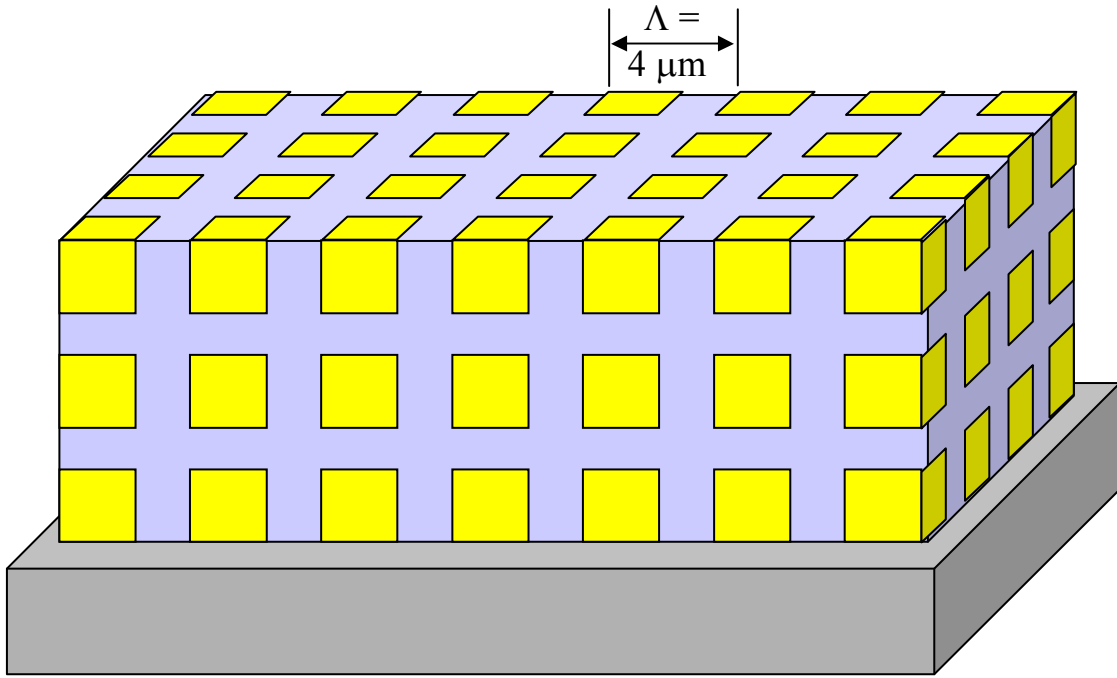


Fig. 1: Sketch of cubic array of cubes

## 2. BACKGROUND

Sandia National Laboratories has been building log-pile photonic bandgap structures<sup>3</sup> for several years using lithographic processes typically used in microchip fabrication. These PBGs operate in the mid-IR with a band edges that vary from  $2\mu\text{m}$  to longer wavelengths as required by application. A photomicrograph<sup>3</sup> of a logpile PBG is shown in Fig. 2.

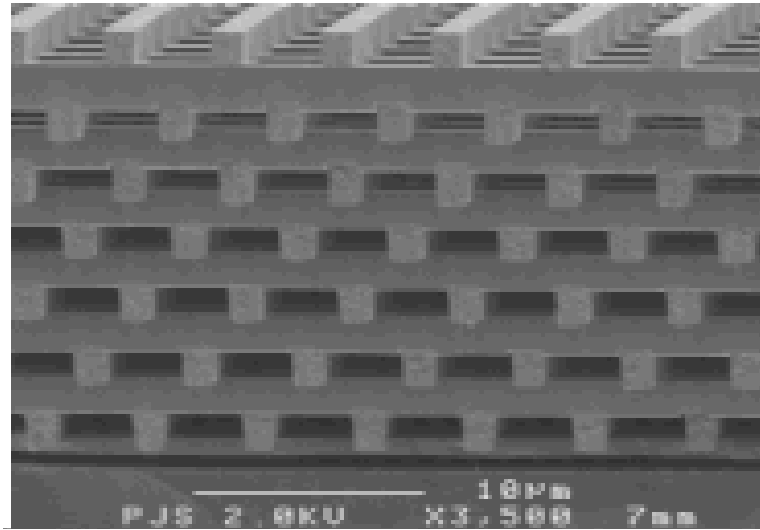


Fig. 2 Photomicrograph of a standard logpile PBG<sup>4</sup>

A metal 3-D PBG structure that is three unit cells thick has nearly the same properties as one that is infinitely thick. Thus a three-unit cell metal PBG structure will achieve good performance while requiring a reasonable fabrication time. A logpile structure that is three unit cells thick requires twelve layers of logs, each one requiring alignment of the mask to the previous structure and a long sequence of chemistry steps, followed by chemical-mechanical polishing. This fabrication process is time-consuming but quite mature. With 150-mm wafers covered with closely spaced 25x25-mm patches of PBGs can be fabricated with high yield. However, this process is quite time-consuming if one needs several square meters of material, which is why we have been seeking a more efficient fabrication process.

Another limitation of the lithographic process is associated with feature size. Pushing toward smaller feature sizes that would move the bandgap toward shorter wavelengths requires higher resolution lithography. While this is available it is very expensive. For example, if a cutoff wavelength of 500nm were needed, the log cross-sections would have to be around 70nm, both in the plane of the surface and perpendicular to it.

For these reasons we have sought other methods of making large pieces of photonic bandgap material. Switching from the logpile architecture to a cubic array of cubes was the first step. It increases the minimum feature size relative to the unit cell and thus the wavelength of operation. For a logpile, the cross-section of the logs is one-fourth of the unit cell size (i.e. 1 $\mu$ m logs in a 4 $\mu$ m unit cell). For a cubic array of cubes, the cube is 5/8<sup>th</sup>s of the unit cell dimension. Thus to make a PBG with a 500nm cutoff wavelength, 175nm cubes would be needed which is well within the range of nano-imprinting and standard projection lithography versus 70nm logs. Also the thicknesses of the cube layers have looser tolerances than do the logs in a logpile.

Note that LIGA can be used to create a "tilted logpile" PBG structures. Such an approach is also being pursued at Sandia. See SPIE 2006 Annual meeting paper<sup>4</sup> for details.

### 3. DEVICE FABRICATION

We have identified two matrix materials for this application. Both BCB and low a low-molecular weight polyethylene are sufficient to demonstrate the cubic array photonic crystal structure. Polyethylene has a reasonable refractive index ( $n \approx 1.5$ ) and relatively good transmission in the thermal IR. While BCB is not as transmissive in the mid-IR as polyethylene, its process conditions are well understood.<sup>5</sup> Either polyethylene or BCB can be used for the production of cubic arrays in the visible/near-IR. To our knowledge no-one had spun polyethylene before so a method of spin casting had to be developed to produce layers a few microns thick. The basic process involves dissolving the polyethylene in cyclotene and xylene to reduce the viscosity sufficiently to allow spinning.

For the lithographic processing, we unsuccessfully tried to use standard wet chemistry. Unfortunately, both the BCB and the polyethylene were damaged by the wet lithographic processing, as well as the (wet) metal liftoff processing, and the electroplating. Our first fabrication attempt started with evaporation of a thin Ti/Au seed layer on the substrate to be used as a seed layer for electroplating. Photoresist was spun onto the seed layer, patterned, and then transformed into a mold using standard photolithography chemistry. Cubes were gold plated into the resist pattern prior to stripping the photoresist using either acetone or oxygen plasma. Both processes resulted in delamination of the underlying polymer film required to fill the matrix. Further investigations lead us to believe that the polyethylene film under the resist layer was absorbing the plating solution and delaminating from the substrate.

Metal liftoff processes were also unsuccessful. The metal liftoff was attempted using evaporated Ti/Au and a developer soak that did not aggressively attack BCB or polyethylene films beneath the resist. However, polyethylene films melted during the evaporation process causing bubbles and voids to form in the die. This resulted in the production of large defects in the lattice and thereby making alignment of the next layer impossible. We then switched to the new scheme detailed below and sketched in Figure 3.

New dry process:

1. First a gold layer is evaporatively deposited on the previously completed layers (or on the bare substrate).
2. A thermal imprint resist is spun on the gold layer and patterned into an array of cubes that will act as a soft mask for creating gold cubes in the metal layer underneath
3. A beam of energetic particles that sputters away the gold not covered by resist, leaving a 2D array of cubes, which are destined to become part of a cubic array of cubes PBG.
4. Note that all of these processes are dry so they don't cause swelling or bubble formation in either the BCB or polyethylene.

A process flow diagram for the fabrication of the cubic array of cubes is shown in Fig. 3. Substrates were metalized with 50 Å of Ti and 2000 Å of Au using physical vapor deposition. Nanonex's NXR-1010 resist was spun and imprinted using an EV520 wafer bonder. The substrate was then sputter-etched in a plasma chamber with argon until the exposed gold was completely removed. The imprint resist was then etched away in an argon plasma. After the etching is completed, a 4μm thick BCB (or polyethylene) film was spun over the substrate, immersing the layer of cubes. The polymer suspension matrix provides an IR-transparent media between each layer of suspended gold structures. The process was then repeated for the subsequent layers.

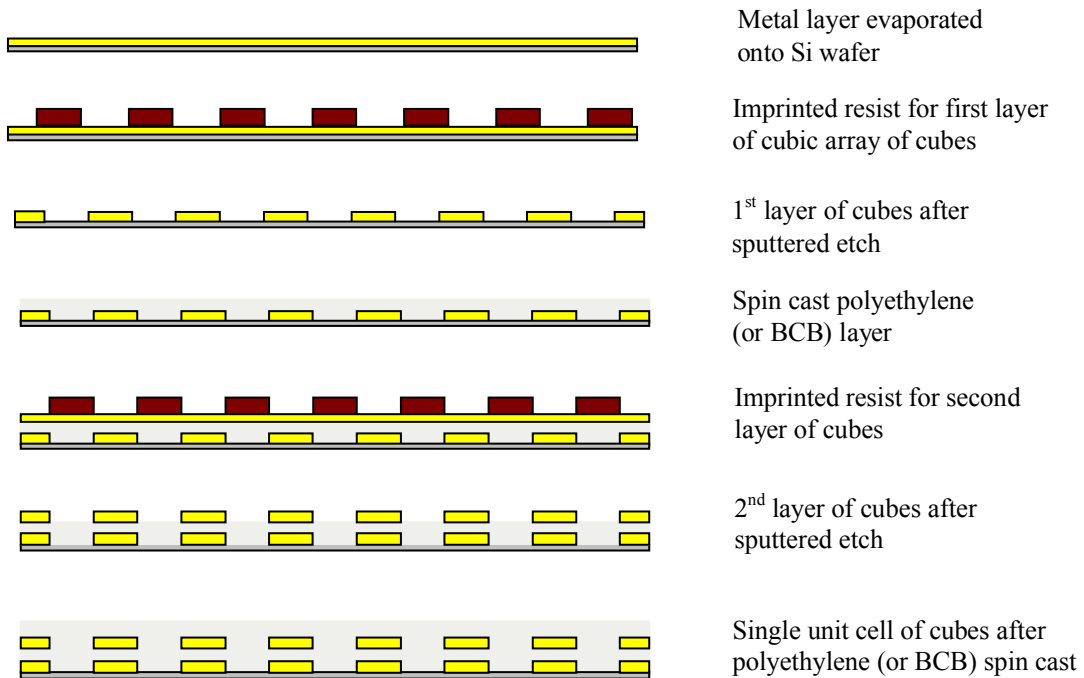


Fig. 3: Process flow diagram for fabrication of cubic array of cubes

The scanning electron microscope images in Fig 4a-4d show the thermal-IR PBG at various stages during the fabrication process. Figure 4a shows the PBG structure after two layers of cubes have been created and filled with BCB. Figure 4b shows the photoresist structure after the exposed gold was sputtered away but before being stripped. Figure 4c is a view of the cube structure after stripping. Figure 4d is a top view of the cubes after they have been filled with the BCB.

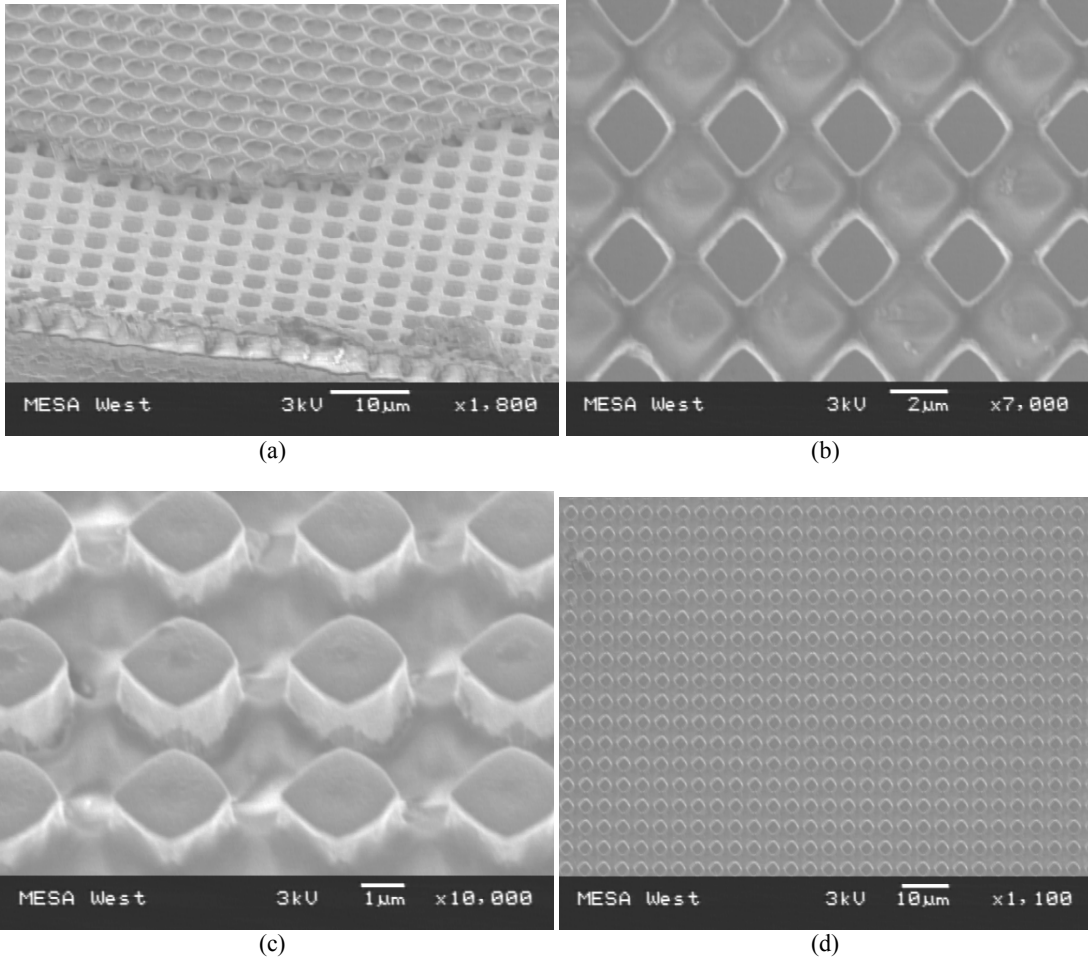


Fig. 4: SEM images of the cubic array of cubes: (a) cross section showing dark gold structures embedded in polyethylene, (b) Etched gold prior to imprint resist strip, (c) etched gold structures after strip, (d) top down view of final structure after filling with BCB

#### 4. SIMULATION AND TESTING OF THE THERMAL-IR CUBIC ARRAY OF CUBES

Analysis of the cubic array of cubes structure was performed using rigorous coupled wave analysis (RCWA). The refractive index value for the low-density polyethylene was assumed to be 1.5. Published values for the refractive index of gold were used. All simulations assume square cubes with perfect layer-to-layer alignment, unless otherwise noted. The array period is 4  $\mu\text{m}$ , the cube width is 2.5  $\mu\text{m}$ , and the cube height is 0.5  $\mu\text{m}$ . Two reflection profiles for normal incidence are shown in Figure 5a. The red one assumes perfect alignment between the two layers of cubes. The green curve shows the results of 1  $\mu\text{m}$  of decenter in both the x and y directions.

As shown in Fig. 5b, there are only two layers of cubes in our first PBG structure. This structure has a full three band gap because it is “one unit cell” thick. We felt that testing the first structure created with a complete band gap would be highly instructive. A four-layer structure (three unit cells thick) has been completed and awaits testing. We should also note that the cubes are arranged in a diamond pattern as seen in the SEM (Figs. 4b & 4c). We expect this to change the bandgap slightly.

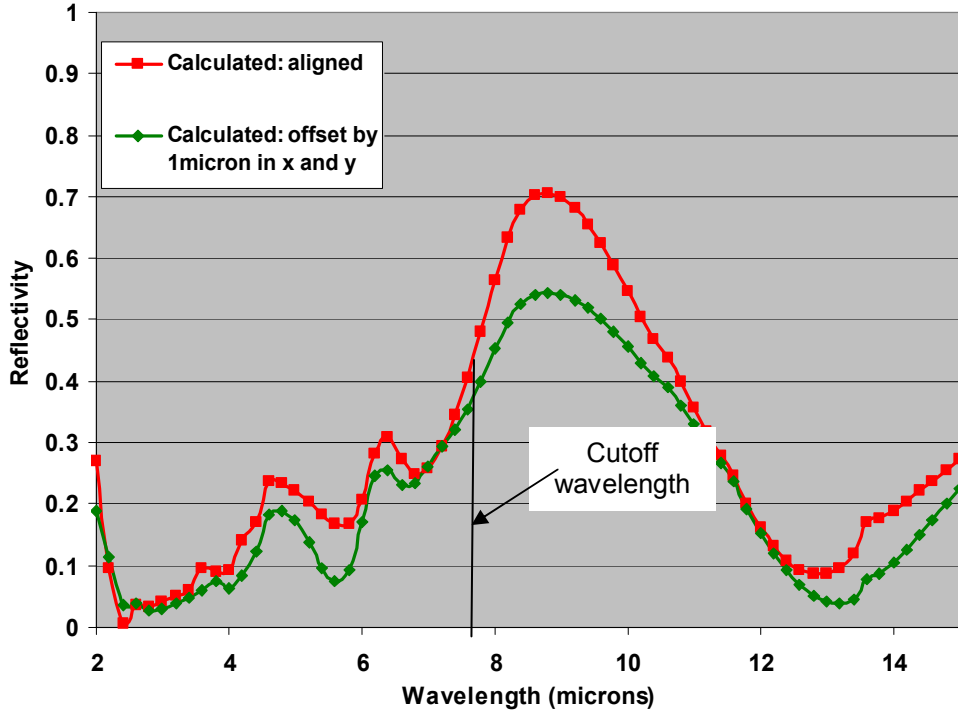


Figure 5a: Calculated reflectivity of a cubic array of cubes with two layers of cubes as shown in Fig. 5b

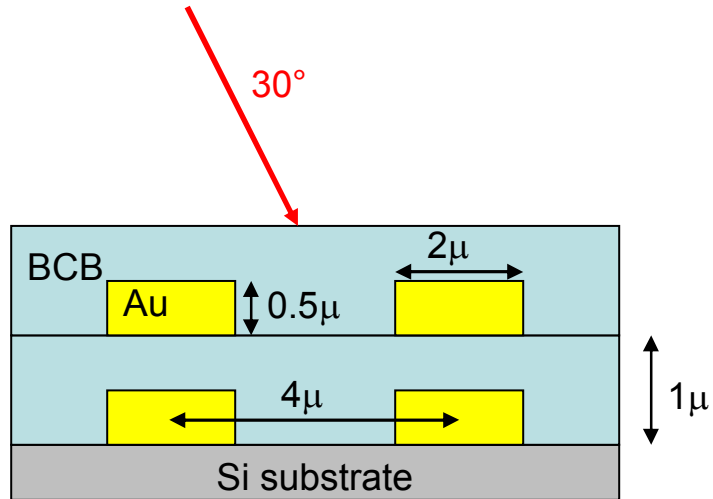


Fig. 5b: Sketch of 2-layer cubic array of cubes.

Details concerning the analysis: The refractive indices of the gold and silicon were found in Palik. The refractive index of BCB was measured to be  $n=1.5$ . The polyethylene was assumed to be the same. Currently we are uncertain of sample's alignment layer-to-layer. The green curve (Fig. 5a) shows that if there is modest misalignment, there will still be a band gap though the peak reflectivity will be reduced.

#### Measurements of the thermal-IR PBG

Figure 6 shows the measured reflectivity curve for a cubic array of cubes that is two layers thick. The angle of incidence for the radiation was  $30^\circ$  off normal. This structure is one unit cell thick, the unit cell being the zone between the centers of the two layers of cubes.

We note that the calculated and measured cut-off wavelengths differ (Fig. 5a & 6). The calculated cutoff is about  $7\mu\text{m}$  while the measured one is nearer to  $8.5\mu\text{m}$ . We will be reviewing the experiment and refining the analysis over the next few months. For example, the polyethylene could have a lower density than we expect so the refractive index could be lower than 1.5. Also, the Ti layer may have different optical properties than the gold. Regarding the analysis, the shapes of the fabricated diamonds (cubes) have rounded corners in the cross-section seen in Figs 4a-4d. The third dimension may also show rounded profiles. We believe these as yet undetermined parameters account for the differences between analysis and experiment.

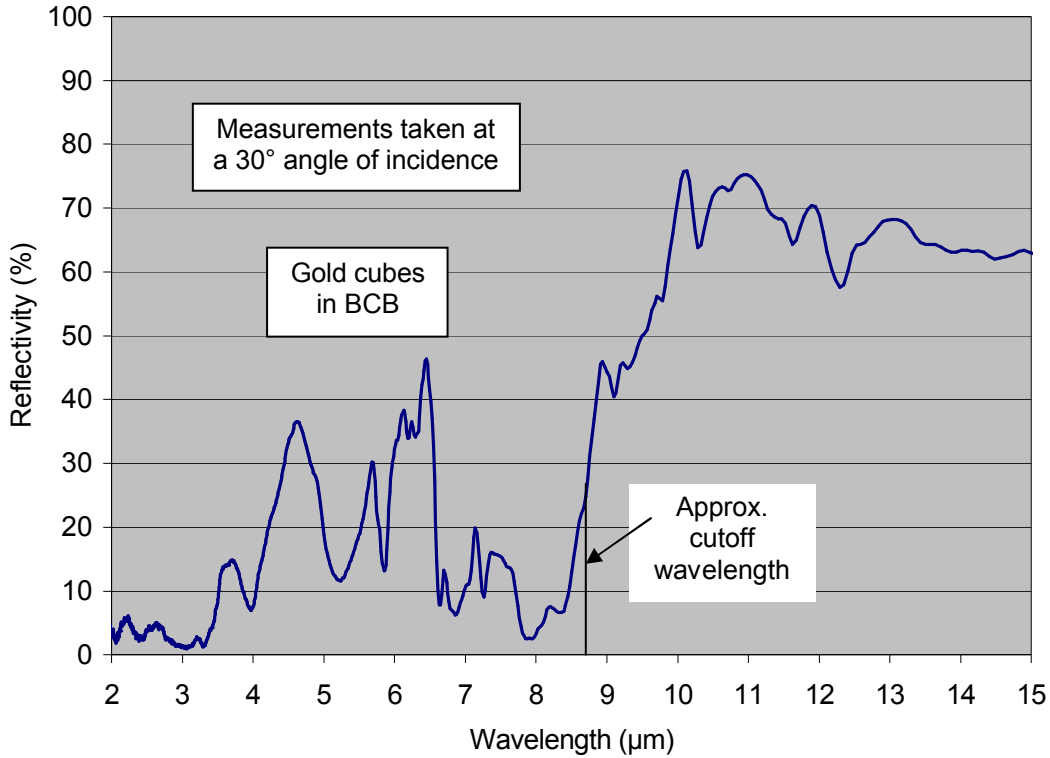


Fig. 6: Measurement of the specular reflectance of a 2-layer, Thermal-IR cubic array of cubes PBG

#### Details about the measurements

All of the measurements in this paper were taken with a Thermo-Nicolet Magna-IR 860 FTIR spectrometer. For the mid-IR PBG sample discussed above, a DTGS detector was used for the full  $2.0\text{-}15.0\mu\text{m}$  range. The reflection measurement referenced a gold-coated mirror, with an assumed reflectance of 100%. Both the reflectance measurements discussed above and below were made at a  $30^\circ$  AOI, making use of a focusing mirror, which resulted in a small range of AOI.

For the near-IR PBG sample discussed below, a Si detector was used for the  $0.42\text{-}1.1\mu\text{m}$  range, and a MCT-A detector for the  $1.1\text{-}2.0\mu\text{m}$  range. The reflection measurement referenced an aluminum mirror which had a nominal 92% reflectance. The data were corrected for the  $<100\%$  reflectance of the mirror by dividing the raw reflectance data by 0.92. The transmission measurement was made using a focusing mirror at normal incidence, which, like the reflectance measurement, resulted in a small range of AOI.

## 5. VISIBLE/NEAR-IR SQUARE ARRAY OF CUBES

We have only recently started building a visible/near-IR cubic array of cubes. As of this writing, we have only made a single layer of "cubes". Figure 7 is a SEM of the resist that has been imprinted with the nano-imprinter mask. Note that the "diamonds" are the part of the resist that is left behind to protect the gold from the sputter etch.

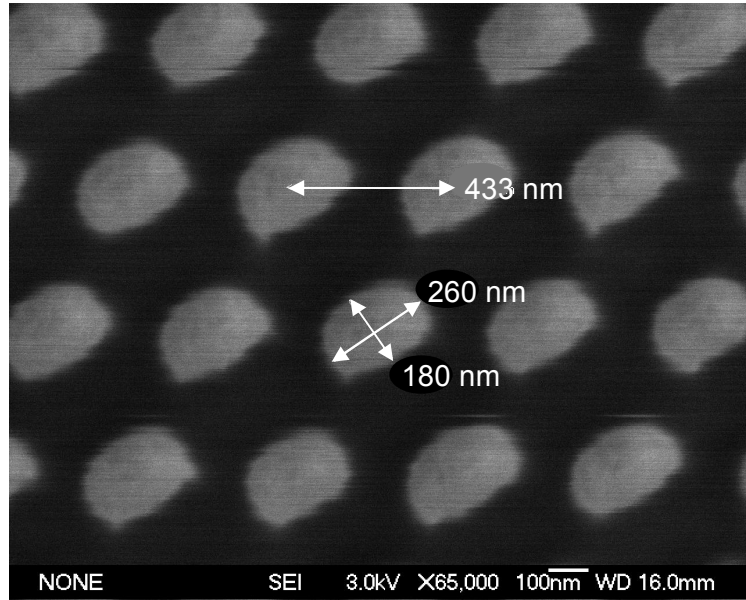


Fig. 7: Visible/Near IR 2-D Array of Cubes Mask– This is the “Imprinted Resist” in the Process Flow Diagram shown in Fig. 3.

### Analysis and measurement of the visible/near-IR layer of cubes:

RCWA was used to calculate the reflectivity, transmission, and absorption of the near-IR planar array of cubes. Published values for the refractive index were used for the sapphire substrate. The parameters used are shown in Figure 8. The polyethylene layer was assumed to have a refractive index of  $n = 1.5$  across the wavelength range. Reflection, transmission, and absorption are shown in Figure 9 for illumination at  $30^\circ$  incidence.

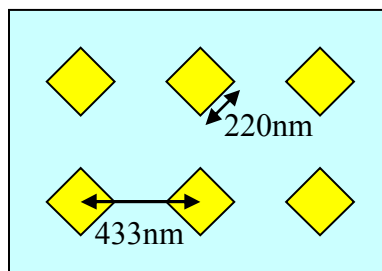


Fig. 8: Top view of simulated near-IR design. Depth of cubes is 200nm.

Figure 10 shows the measurements performed on the square array of cubes, which is the first layer of a cubic array of cubes designed to operate in the visible/near-IR region of the spectrum. Differences between the simulated and modeled results are due in part to the different configurations of the two structures (square vs. triangular arrays).

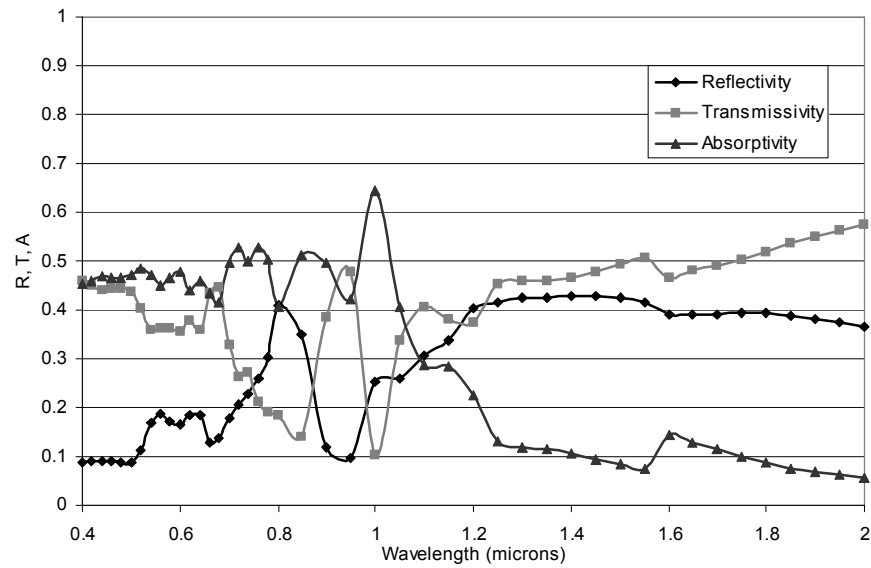


Fig. 9: RCWA calculations of the reflection, transmission, and absorption of a 1-layer thick "square" array of cubes with a  $\Lambda = 433\text{nm}$  unit cell dimension.

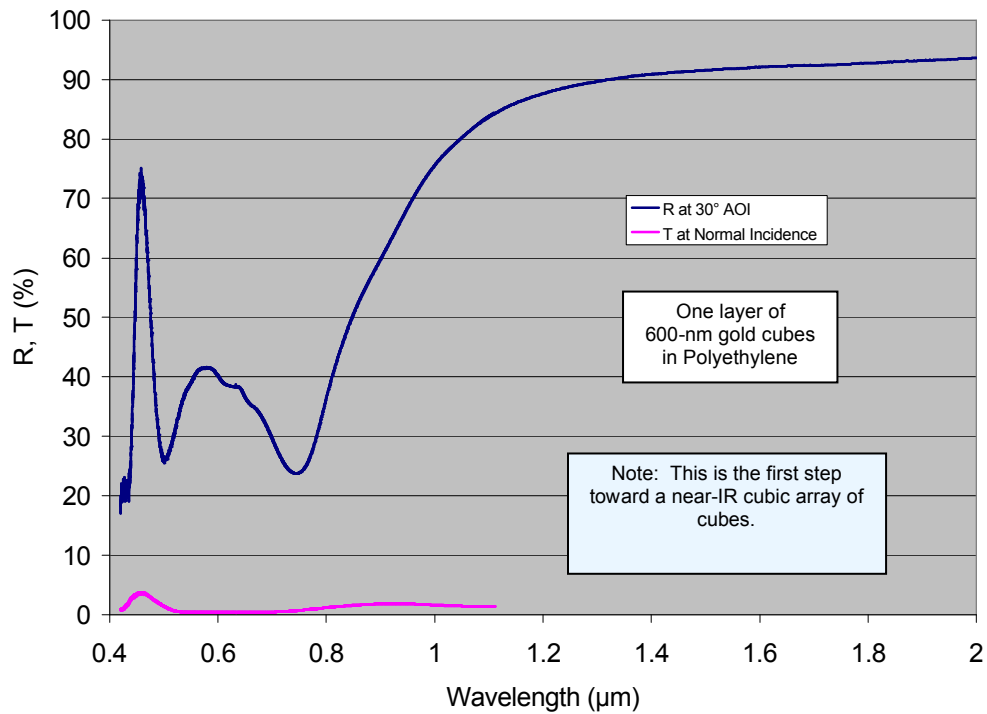


Fig. 10: Reflectivity and Transmittance of a single layer near-IR cubic array in polyethylene.

## 6. SUMMARY AND FUTURE WORK

- Photonic crystals with a cubic array of cubes architecture have been modeled, fabricated, and tested.
- The patterning was done with an imprinter and then “dry” processing was used.
- We have shown the capability to fabricate structures with periods of 433nm.
- This process can be scaled, thus allowing large pieces (areas) of photonic bandgap material to be fabricated.
- We will begin fabrication of a thermal-IR PBG and a visible/near-IR PBG, each with four layers during the fall of 2006.

## 7. REFERENCES

1. M.U. Pralle, et.al, *Photonic crystal enhanced narrow-band infrared emitters*, App. Phys. Let. V.81,no.25, 12/16/2002 (cubic array of cubes)
2. Matthias, S; Muller, F; Gosele, U, *Characterization of simple cubic three-dimensional photonic crystals with complete photonic bandgaps* SPIE; v.5733, p.12-22 (2005)
3. J.G. Fleming, et. al, *All-metallic three-dimensional photonic crystals with a large infrared bandgap*, Nature, Vol.417, p.52, 5/2/2002
4. J.D. Williams, et. al, *Tilted logpile photonic crystals using the LIGA technique*, Proc. SPIE 6289 (2006).
5. K.-I. Kim, et.al, *Packaging of RF MEMS devices using LTCC substrate and BCB adhesive layer*, J. Micromech. Microeng. 16, 150-156 (2006).